Supporting Information

Wang et al. 10.1073/pnas.1615718114

SI Text

Calculations of the Summer Surface Nitrate Concentration in the Southern Ocean

Rayleigh Model. When phytoplankton consume nitrate, they preferentially assimilate ^{14}N relative to ^{15}N, leaving the residual nitrate pool enriched in ^{15}N and yielding a relationship between the $\delta^{15}N$ of the accumulated organic N (integrated product) and the degree of nitrate consumption/nitrate utilization (37). Thus, in ocean regions where surface nitrate is not completely consumed and there is a strong temporal separation of nitrate supply and nitrate consumption, such as the Southern Ocean (38, 39), the $\delta^{15}N$ of the accumulated organic N is an approximate proxy for the degree of nitrate consumption. Over the course of a year, the organic N export/sinking flux should equal the consumed nitrate, so that the $\delta^{15}N$ of the sinking flux can be described by the Rayleigh model's approximate integrated product equation:

$$\delta^{15}N_{integrated} = \delta^{15}N_{initial} + \epsilon \times \frac{f \times \ln f}{1-f}, \quad [S1]$$

where $\delta^{15}N_{initial}$ is the nitrate $\delta^{15}N$ before nitrate consumption; ϵ is the isotope effect of nitrate consumption (positive value means the product is depleted in ^{15}N relative to the substrate); and f is the fraction of remaining nitrate. The residual nitrate $\delta^{15}N$ is approximated by the following:

$$\delta^{15}N_{NO_3^-} = \delta^{15}N_{initial} - \epsilon \times \ln f. \quad [S2]$$

Deep-sea corals feed on organic matter that derives from this sinking flux, and the $\delta^{15}N$ of deep-sea coral-bound organic N has been shown to be a good proxy for the $\delta^{15}N$ of the sinking flux in the modern ocean (14).

Below, we use the Rayleigh model to calculate the surface nitrate concentration in the Southern Ocean over the past 40 kyr, based on our three coral $\delta^{15}N$ datasets and the published foraminifera and diatom $\delta^{15}N$ datasets in Fig. 3 (12, 13). Because diatoms, foraminifera, and corals are three distinct groups of organisms at different trophic levels, we normalize each $\delta^{15}N$ dataset to their modern values by subtracting the modern $\delta^{15}N$ values from each record, yielding the $\delta^{15}N$ anomaly (Fig. 3). We then apply the Rayleigh model to each dataset and compute the surface nitrate concentration for each of the five datasets, taking into account changes in the initial nitrate concentration and $\delta^{15}N$ as described below.

AZ Summertime Surface Nitrate Concentration Since 40 kyr Ago. In the AZ, both the coral and diatom records show on average 4–5‰ higher $\delta^{15}N$ during the LGM than the late Holocene (Fig. 3*A*). Applying the Rayleigh model to the AZ surface ocean:

$$\delta^{15}N_{AZ\text{-}integrated} = \delta^{15}N_{UCDW} + \epsilon_{AZ} \times \frac{f_{AZ} \times \ln f_{AZ}}{1-f_{AZ}}, \quad [S3]$$

$$[NO_3^-]_{AZ} = [NO_3^-]_{UCDW} \times f_{AZ}, \quad [S4]$$

$$\delta^{15}N_{[NO_3^-]AZ} = \delta^{15}N_{UCDW} - \epsilon_{AZ} \times \ln f_{AZ}, \quad [S5]$$

where Upper Circumpolar Deep Water (UCDW) in the AZ is used as the starting nitrate pool [$[NO_3^-]_{UCDW} = 33$ μM; $\delta^{15}N_{UCDW} = 5$‰ (40)]; ϵ_{AZ} is the isotope effect of nitrate consumption in the AZ surface ocean; f_{AZ} is the fraction of remaining nitrate (with a modern value of 0.7); $[NO_3^-]_{AZ}$ is the residual nitrate concentration in the AZ surface; and $\delta^{15}N_{[NO_3^-]AZ}$ is the residual nitrate $\delta^{15}N$ in the AZ surface.

As indicated in Eq. **S3**, $\delta^{15}N_{AZ\text{-}integrated}$ is a function of three variables: $\delta^{15}N_{UCDW}$, ϵ_{AZ}, and f_{AZ}. It is thus important to consider the changes in the other two variables before we attribute the 4–5‰ higher LGM $\delta^{15}N_{AZ\text{-}integrated}$ to a change in the surface nitrate concentration.

For the AZ, the dominant source of nitrate to the winter mixed layer (which sets the initial nitrate concentration and $\delta^{15}N$ of the summer mixed layer) is mixing with and upwelling of UCDW. Thus, to change $\delta^{15}N_{initial}$ in the AZ, one has to change the UCDW nitrate $\delta^{15}N$. One possible way to do this is to change the mean ocean nitrate $\delta^{15}N$. However, although there is a paucity of direct evidence as to mean ocean nitrate $\delta^{15}N$ over glacial–interglacial cycles, the existing data suggest that mean ocean nitrate $\delta^{15}N$ changed very little over the past 40 kyr (41, 42). Given the evidence for N fixation feedbacks (11, 33, 43), the ocean nitrate reservoir has likely been tied to that of phosphate (44), and UCDW nitrate concentration is today similar to the mean deep-ocean value. Thus, major changes in UCDW nitrate concentration are also unlikely. In all of the calculations below, we assume that the nitrate concentration and $\delta^{15}N$ in UCDW have remained constant over the past 40 kyr.

A change in ϵ_{AZ} during the LGM is also possible, given the previous finding that ϵ_{AZ} varies as a function of mixed layer depth in the Southern Ocean (45). We can explore the possible contribution of changing ϵ_{AZ} to the 4–5‰ higher LGM $\delta^{15}N_{AZ\text{-}integrated}$. For a given value of $\delta^{15}N_{UCDW}$, a contour plot of $\delta^{15}N_{AZ\text{-}integrated}$ as a function of ϵ_{AZ} and f_{AZ} can be generated using Eq. **S3** (Fig. S8). It shows that, within the range of observed isotope effect of nitrate assimilation in the modern ocean (45), the $\delta^{15}N_{AZ\text{-}integrated}$ is more sensitive to changes in f_{AZ} than in ϵ_{AZ}, especially when the surface nitrate consumption is high. The modern AZ has an average f_{AZ} value of ∼0.7 and a ϵ_{AZ} value of ∼6‰ (45). Because ϵ_{AZ} during the spring-to-fall nitrate drawdown is unlikely to be lower than 4‰ (46), the maximum increase in LGM $\delta^{15}N_{AZ\text{-}integrated}$ caused by a lower ϵ_{AZ} is less than 2‰ and most likely less than 1‰. When converting the $\delta^{15}N$ anomaly records into the surface nitrate concentration records, we use a ϵ_{AZ} value of 6‰ and assume that ϵ_{AZ} in the AZ has not changed over the past 40 kyr.

SAZ Summertime Surface Nitrate Concentration Since 40 kyr. In the SAZ, the coral and foraminifera records also show 4–5‰ higher $\delta^{15}N_{integrated}$ during the LGM than the late Holocene (Fig. 3*B*). As for the AZ above, we consider here the possibility of changes in the concentration of the nitrate supply, $\delta^{15}N_{initial}$, and nitrate assimilation isotope effect, and their role in the 4–5‰ higher LGM $\delta^{15}N_{integrated}$ in the SAZ.

In contrast to the AZ, the modern SAZ thermocline water has two primary sources of nitrate and at least three sources of water. First, Ekman transport carries AZ surface water into the SAZ, and this water contains the nitrate remaining from nitrate assimilation in the AZ (18). This nitrate enters the SAZ at the surface, but it is mixed throughout the deep wintertime SAZ mixed layer, including the depths of Subantarctic Mode Water. Second, the SAZ thermocline exchanges waters with the low-latitude upper ocean. This water has a very low nitrate concentration and effectively dilutes the nitrate in the SAZ thermocline (47). Third,

diapycnal mixing of the SAZ thermocline with underlying Antarctic Intermediate Water (AAIW) and UCDW incorporates nitrate with a high concentration (33 μM) and relatively low $\delta^{15}N$ (~5.5‰ in the SAZ). It has been estimated that the Ekman transport contributes to 60–70% of the SAZ thermocline nitrate in the modern ocean, with diapycnal mixing making up the remaining 30–40% (48).

We use a three–end-member mixing model to simulate the mean concentration and $\delta^{15}N$ of the gross nitrate supply to the SAZ thermocline/wintertime mixed layer. Because the low-latitude water contains no nitrate and because we have no reason to expect its contribution of water to vary relative the contribution from UCDW, we combine the low-latitude water end-member with the UCDW end-member. In this way, the three–end-member mixing model is simplified to a two–end-member mixing model. Thus, we use the following proportions of water from the three sources described above: 60% from the Ekman transport and 40% from UCDW (Fig. S5).

Eqs. **S6** and **S7** describe the mixing results of the SAZ thermocline nitrate:

$$\left[NO_3^-\right]_{\text{SAZ-thermocline}} = \left[NO_3^-\right]_{\text{UCDW}} \times f_{\text{AZ}} \times b + \left[NO_3^-\right]_{\text{mixedUCDW}} \times (1-b), \quad \textbf{[S6]}$$

$$\delta^{15}N_{\text{SAZ-thermocline}} = \delta^{15}N_{\text{AZ}[NO_3^-]} \times \frac{\left[NO_3^-\right]_{\text{UCDW}} \times f_{\text{AZ}} \times b}{\left[NO_3^-\right]_{\text{SAZ-thermocline}}} + \delta^{15}N_{\text{mixedUCDW}} \times \frac{\left[NO_3^-\right]_{\text{mixedUCDW}} \times (1-b)}{\left[NO_3^-\right]_{\text{SAZ-thermocline}}}, \quad \textbf{[S7]}$$

where $[NO_3^-]_{\text{SAZ-thermocline}}$ is the nitrate concentration in the SAZ thermocline; b is the SAZ water fraction from the AZ [set to a constant value of 0.6 (48)]; $[NO_3^-]_{\text{mixedUCDW}}$ is the UCDW nitrate concentration after mixing with low-latitude water [set to a constant value of 18 μM (17, 18)]; $\delta^{15}N_{\text{mixedUCDW}}$ is the $\delta^{15}N$ of the UCDW nitrate input to the SAZ [set to a constant value of 5.5‰ (17, 18)].

This mixing yields a modern SAZ thermocline/winter mixed layer nitrate concentration of ~20 μM, which is assumed to be drawn down to ~10 μM by nitrate assimilation in the SAZ (18). Holding these water mixing proportions constant, we estimate the changing SAZ thermocline nitrate concentration from 40 kyr ago to the present (Fig. S6). One clear oversimplification is that summertime AZ conditions are used to calculate the year-round nitrate concentration coming from the AZ. However, during the LGM, the winter-to-summer nitrate concentration decline in the AZ was probably very weak (Fig. S5) such that our approach is a reasonable simplification so far as the effect of the AZ on the SAZ nitrate concentration is concerned.

The reconstructed nitrate concentration for the gross nitrate supply to the SAZ provides the initial nitrate concentration for the Rayleigh model calculation (Eqs. **S8** and **S9**):

$$\delta^{15}N_{\text{SAZ-integrated}} = \delta^{15}N_{\text{SAZ-thermocline}} + \epsilon_{\text{SAZ}} \times \frac{f_{\text{SAZ}} \times \ln f_{\text{SAZ}}}{1-f_{\text{SAZ}}}, \quad \textbf{[S8]}$$

$$\left[NO_3^-\right]_{SAZ} = \left[NO_3^-\right]_{\text{SAZ-thermocline}} \times f_{\text{SAZ}}, \quad \textbf{[S9]}$$

where ϵ_{SAZ} is the isotope effect of nitrate assimilation in the SAZ [set to a constant value of 8.5‰ (18)]; and f_{SAZ} is the fraction of residual nitrate in the SAZ surface (with a modern value of 0.5).

The same mixing model also provides a reconstruction of the $\delta^{15}N$ of the gross nitrate supply to the SAZ (Eq. **S7** and Fig. S6). Fig. S3*B* uses this as well as the calculated nitrate concentration described above as the initial nitrate $\delta^{15}N$ and concentration for the Rayleigh model calculation. The $\delta^{15}N$ of the gross nitrate supply to the SAZ from all sources tends to decrease under the LGM case of nearly complete nitrate consumption in the AZ (Figs. S5 and S6). Relative to UCDW, the AZ surface elevates the $\delta^{15}N$ of the nitrate supply to the SAZ. When AZ nitrate concentration is very low, it can no longer play this role, and the $\delta^{15}N$ of the nitrate supply to the SAZ collapses on the $\delta^{15}N$ of UCDW nitrate.

The calculation of the $\delta^{15}N$ of the nitrate supply to the SAZ is more uncertain than that of the concentration of the nitrate supply. A high degree of nitrate consumption in the AZ surface during the LGM would by itself raise the $\delta^{15}N$ of the nitrate to be transported northward into the SAZ. However, the resulting low concentration of nitrate in the summer AZ means that its wintertime mixing with underlying water could erase much of this $\delta^{15}N$ elevation. Accounting for such dilution effects is inherently uncertain. Nevertheless, in the calculations, the AZ is not a major nitrate source to the SAZ during the LGM, and so the $\delta^{15}N$ of this minor nitrate source has little effect on the $\delta^{15}N$ of the nitrate supply to the SAZ at this time.

Similar to the AZ, a change in ϵ_{SAZ} would lead to changes in $\delta^{15}N_{\text{SAZ-integrated}}$. However, in comparison with the AZ, a given change in ϵ_{SAZ} will contribute less to the higher LGM $\delta^{15}N_{\text{SAZ-integrated}}$ in the SAZ because the average surface nitrate consumption is relatively high (~50%) even in the modern SAZ (Fig. S8).

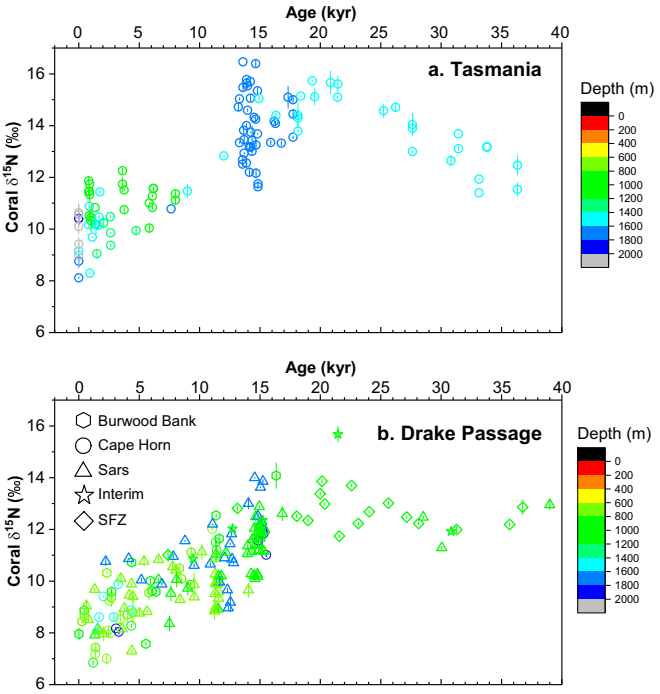

Fig. S1. Nitrogen isotopes of corals from Tasmania (*A*) and Drake Passage (*B*), with the colors indicating the collection depth of each coral. The error bars (±1σ) are calculated from two to three replicates from the same subsample of each coral septum.

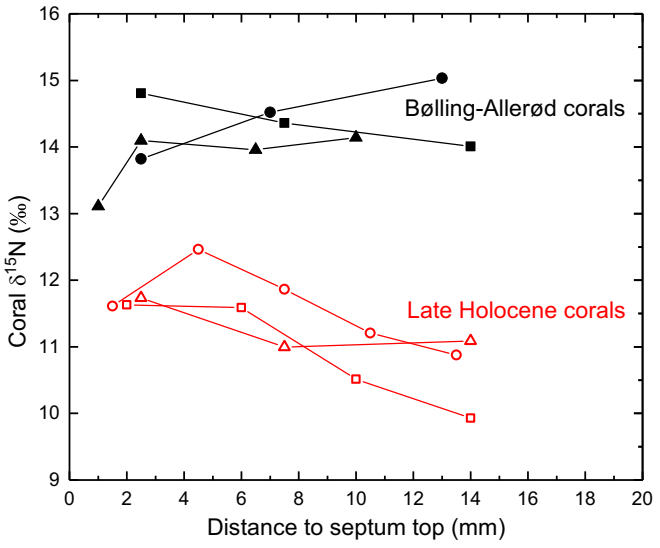

Fig. S2. Tasmanian SAZ coral $\delta^{15}N$ variation on single septa along the growth direction. Each symbol indicates one individual coral [filled symbols: late Holocene corals; open symbols: Bølling–Allerød (13–14 kyr) corals].

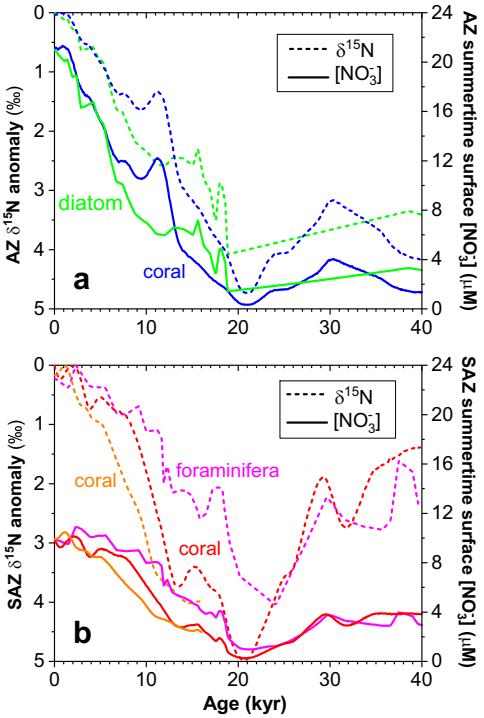

Fig. S3. Comparison of coral $\delta^{15}N$ records with the sedimentary microfossil $\delta^{15}N$ records as in Fig. 3, and the reconstructed histories of AZ and SAZ summertime surface nitrate concentration. (*A*) Comparison of the Drake Passage AZ coral $\delta^{15}N$ mean record with the PS75/072-4 AZ diatom $\delta^{15}N$ record ($\delta^{15}N$ anomaly was calculated by subtracting the modern or core-top $\delta^{15}N$ values from each record) (13) and the calculated AZ summertime surface nitrate concentration over the past 40 kyr based on the Rayleigh model (*SI Text*). (*B*) Comparison of the SAZ coral $\delta^{15}N$ records with the ODP Site 1090 SAZ foraminifera $\delta^{15}N$ record (12) and the calculated SAZ summertime surface nitrate concentration based on the Rayleigh model and the reconstructed concentration and $\delta^{15}N$ of the nitrate supply to the SAZ (*SI Text* and Figs. S5 and S6).

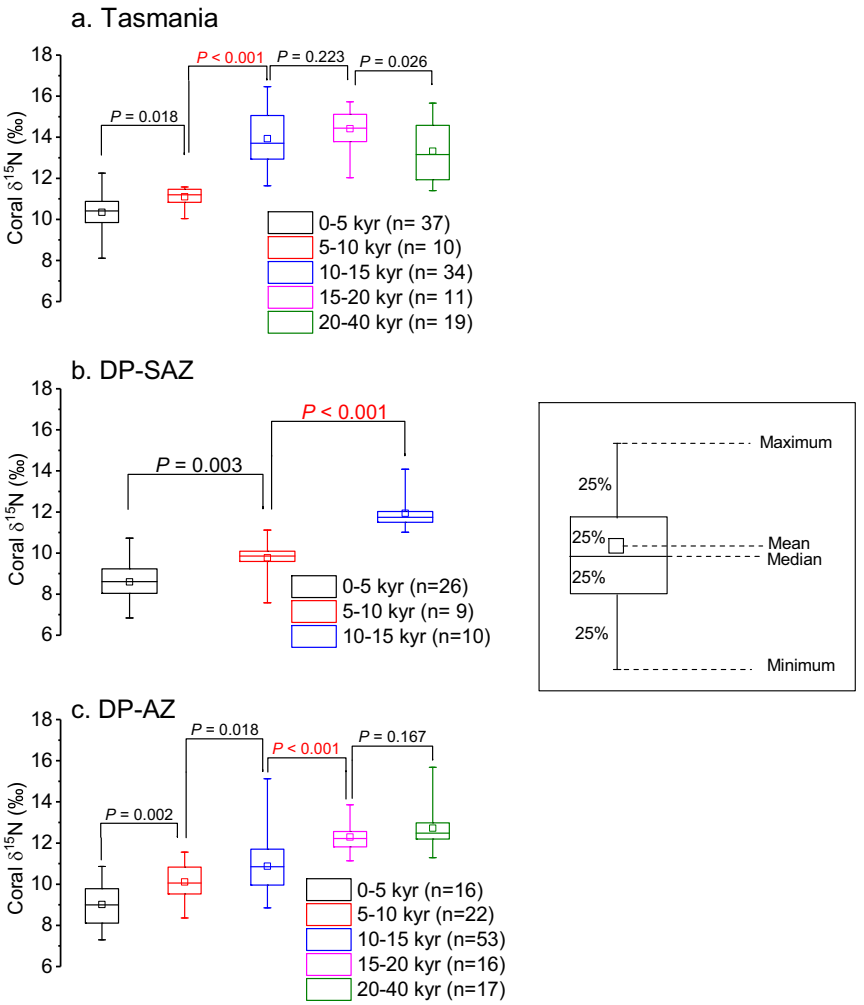

Fig. S4. Box plots of coral $\delta^{15}N$ [(*A*) Tasmania; (*B*) Drake Passage SAZ (DP-SAZ); (*C*) Drake Passage AZ (DP-AZ)] for each 5-kyr bin (except for 20–40 kyr) and *P* values of each two adjacent groups based on Mann–Whitney *U* test (Wilcoxon rank-sum test).

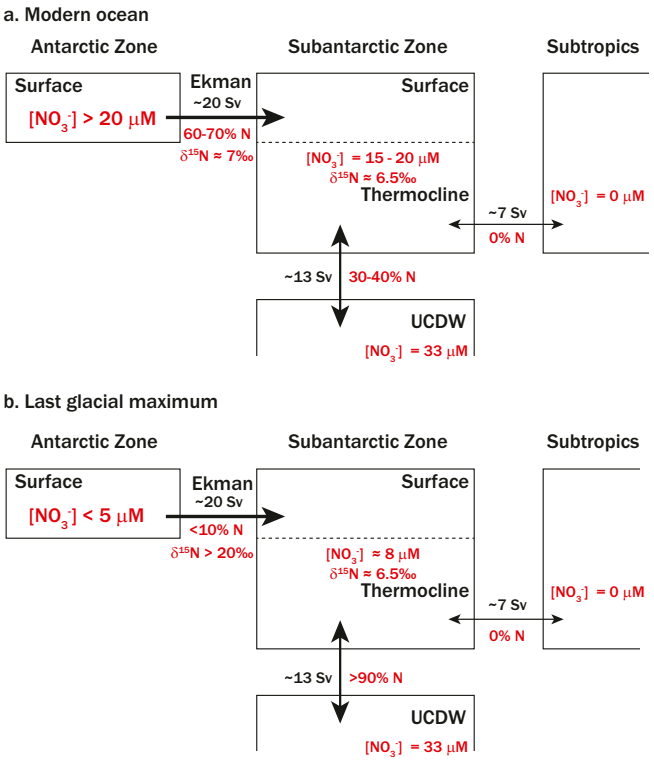

Fig. S5. A schematic showing the impact of AZ processes on the SAZ nitrate concentration and $\delta^{15}N$ and the formulation of this impact with our end-member mixing model. (*A*) In the modern ocean, the surface nitrate concentration is high in the AZ, and the northward Ekman transport transfers a large amount of nitrate to the SAZ, contributing to 60–70% of the gross nitrate supply to the SAZ. (*B*) During the LGM, although the AZ surface nitrate has a high $\delta^{15}N$, the surface nitrate concentration is low in the AZ surface, so the northward Ekman transport thus transfers less nitrate to the SAZ. Under these conditions, the dominant nitrate source in the SAZ is underlying UCDW, which thus has the greatest control on the $\delta^{15}N$ of the net nitrate supply to the SAZ surface.

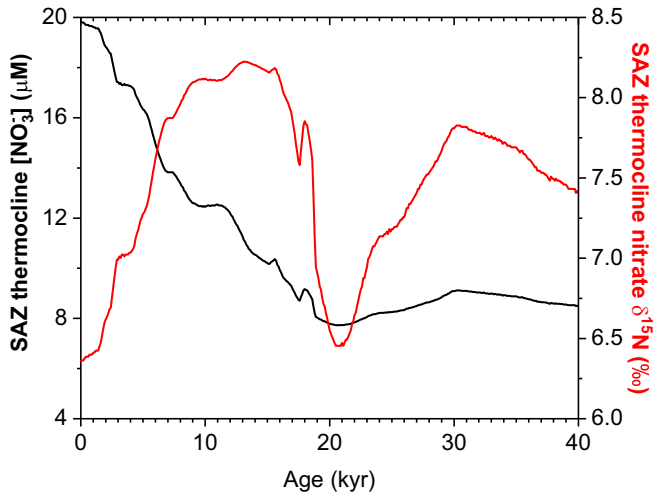

Fig. S6. Calculated SAZ thermocline nitrate concentration and $\delta^{15}N$ from our end-member mixing model. These calculated changes in both the concentration and the $\delta^{15}N$ of SAZ thermocline nitrate are included in the Rayleigh-based reconstruction of SAZ summertime surface nitrate concentration plotted in Fig. S3*B*.

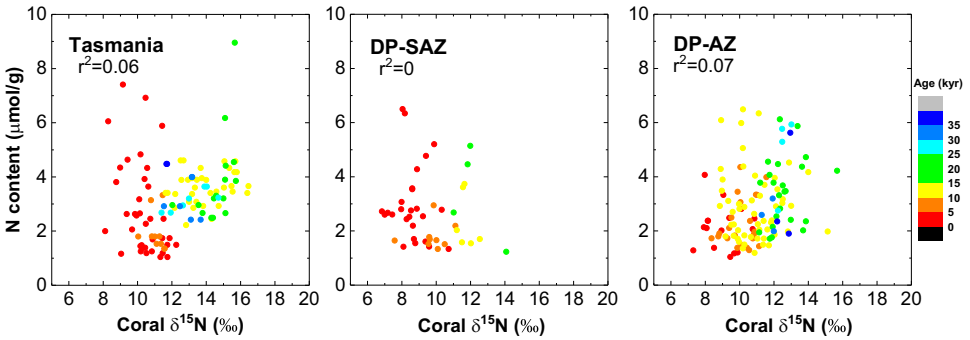

Fig. S7. Comparison of coral δ^{15}N and N content, with samples colored based on age. If there is any tendency in N content as a function of age, it is of increasing N content with age, inconsistent with N loss with time. There is a lack a lack of correlation between N content and coral δ^{15}N (r^2 values shown in *Upper Left*).

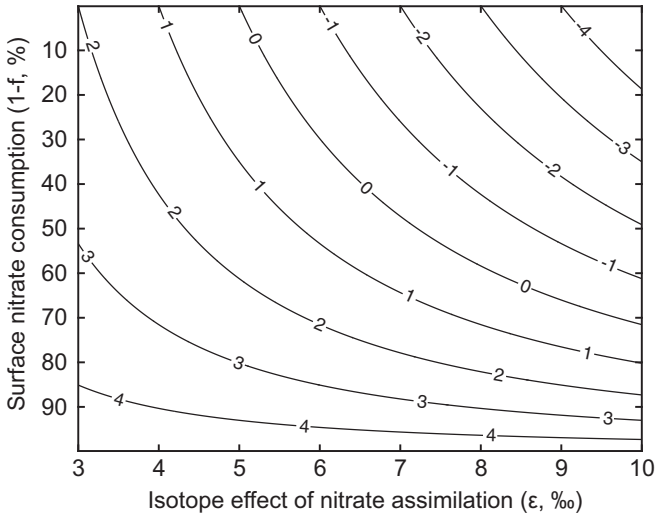

Fig. S8. Contours of the $\delta^{15}N_{AZ\text{-}integrated}$ as a function of ε and $(1-f)$, based on the Rayleigh model (with an initial nitrate δ^{15}N of 5‰ assumed for the calculations shown in this figure). The downward convergence of isolines shows that $\delta^{15}N_{AZ\text{-}integrated}$ is less sensitive to the isotope effect of nitrate assimilation at higher surface nitrate consumption, such that it imposes only a modest to minor uncertainty at nitrate consumption higher than 50%.

Other Supporting Information Files

Dataset S1 (XLSX)
Dataset S2 (XLSX)